Liquid Crystalline Perylene Bisimide Derivatives Bearing Oligosiloxane Moieties

Funahashi, Masahiro

Uemura, Shinobu

(Citation)
Chemistry,8(4):45

(Issue Date)
2026-04-03

(Resource Type)
journal article

(Version)
Version of Record

(URL)
https://hdl.handle.net/20.500.14094/0100503470

chemistry

MDPI

Review

Liquid Crystalline Perylene Bisimide Derivatives Bearing Oligosiloxane Moieties

Masahiro Funahashi [1,2,*] and Shinobu Uemura [3]

[1] Department of Chemical Science and Engineering, Graduate School of Engineering, Kobe University, 1-1 Rokkodai, Nada-ku, Kobe 657-8501, Japan
[2] Research Center for Advanced Membrane and Film Technology, Kobe University, 1-1 Rokkodai, Nada-ku, Kobe 657-8501, Japan
[3] Program in Advanced Materials Science, Faculty of Engineering and Design, Kagawa University, 2217-20 Hayashi-cho, Takamatsu 761-0396, Japan; uemura.shinobu@kagawa-u.ac.jp
* Correspondence: funahashi.masahiro@phoenix.kobe-u.ac.jp

Abstract

Perylene bisimide derivatives are typical *n*-type semiconductors as well as redox-active materials. However, it has been difficult to produce thin films by solution processes because of their low solubilities in organic solvents. Perylene bisimide derivatives bearing oligosiloxane moieties exhibit columnar phases over wide temperature ranges, including room temperature and high solubilities in organic solvents. The columnar phases are stabilized by nanosegregation between crystal-like one-dimensional π-stacks and liquid-like mantle consisting of oligosiloxane moieties. The electron mobility at room temperature exceeded 0.1 $cm^2V^{-1}s^{-1}$ in the ordered columnar phases of perylene bisimide derivatives bearing four disiloxane chains. Uniaxially aligned thin films of the perylene bisimide derivatives bearing oligosiloxane moieties could be produced by a spin-coating method. The spin-coated films of the perylene bisimide derivatives bearing cyclotetrasiloxane rings could be insolubilized via in situ ring-opening polymerization by the exposure of the thin films to trifluoromethanesulfonic acid vapors. Uniaxially aligned thin films of perylene bisimide derivatives bearing an ethylene oxide chain as well as cyclotetrasiloxane rings could be doped in an aqueous solution of sodium dithionate, resulting in an anisotropic electrical conductivity. Polymerized thin films of perylene bisimide derivatives bearing a crown ether ring exhibited electrochromism in electrolyte solutions. These compounds formed 1:1 complexes with lithium triflate, exhibiting columnar phases at room temperature. The nanostructures of the complexes were stabilized by the electrostatic interaction between cationic crown-metal units and triflate anions.

Keywords: liquid crystal; perylene bisimide; electron transport; redox activity; waxy material; interstitial doping; electrochromism; alkaline crown complex

Academic Editors: Igor Alabugin and Matthias Lehmann

Received: 4 March 2026
Revised: 25 March 2026
Accepted: 31 March 2026
Published: 3 April 2026

1. Introduction

Liquid crystals comprising extended π-conjugated units are known as liquid crystalline semiconductors [1–5]. High charge carrier mobilities exceeding 0.1 $cm^2V^{-1}s^{-1}$ have been observed in ordered smectic and columnar phases [6,7]. Temperature-independent charge carrier mobility over a wide temperature range was confirmed, indicating a band-like conduction [8]. Applications to field-effect transistors, light-emitting diodes, and solar cells have been investigated, aimed at solution-processable and flexible devices [9–17].

In the design of liquid crystalline semiconductors, extension of the π-conjugated core is indispensable for efficient carrier transport and red-shift in absorption bands. However, extension of π-conjugated units causes severe problems with decreased solubilities in organic solvents and increased phase transition temperatures due to strong π-π interaction. One approach is the selection of convenient side chains that retain the materials' solubilities but do not perturb π-orbital overlaps at the same time.

Side chains of liquid crystal molecules play significant roles in the appearance of mesophases. Thermal motion of the side chains of liquid crystal molecules inhibits the aggregation of the molecules moderately, assisting the formation of fluidic and soft phases [18]. On the other hand, flexible side chains aggregate each other and promote nanosegregation from rigid core moieties to form lamellar, columnar, and network supramolecular assemblies [19–23].

Typical side chains are linear alkyl chains. Branched alkyl chains are sometimes used for liquid crystal materials with low phase transition temperatures and high solubilities in organic solvents [18]. Oligoethylene oxide chains are also used as hydrophilic units for liquid crystals with electrochemical functions. Oligoethylene oxide chains take a liquid-like disordered conformation, compared to alkyl chains [24–26]. Bulky side chains are effective in increasing the solubility and lowering the phase transition temperature of the LC materials. However, bulky substituents usually inhibit intermolecular aggregation of the π-conjugated units to perturb the efficient intermolecular charge transfer.

We have paid attention to oligosiloxane moieties as a *convenient* side chain. Oligosiloxane side chains have been utilized for side chains of conjugated polymers, promoting crystallization of the π-conjugated chains [27–29]. Ferroelectric liquid crystals bearing oligosiloxane chains exhibited the de Vries type chiral smectic C phase [30–32]. However, the examples of oligosiloxane units used for the side chains of columnar phases were very limited [33]. Si-O bond length is longer than C-C bond length, and the rotation potential around a Si-O bond is lower than that around a C-C bond [34,35]. Oligosiloxane side chains take a liquid-like disordered conformation, similarly to oligoethylene oxide chains; however, unlike hydrophilic oligoethylene oxide chains, they are hydrophobic. They are bulkier than alkyl chains, although nanosegregation between oligosiloxane moieties and rigid cores promotes the formation of smectic and columnar phases, which are favorable for efficient charge carrier transport [36]. In this article, we review a few recent topics of liquid crystalline perylene bisimide derivatives bearing oligosiloxane moieties with softness, efficient electron transport properties, and redox activities.

2. Liquid Crystalline Perylene Bisimide Bearing Oligosiloxane Units

2.1. Oligosiloxane Moiety as a Side Chain Unit and Perylene Bisimide as a Functional Unit

Only a few researchers have synthesized ferroelectric liquid crystals bearing 1,1,1,3,3-pentamethyldisiloxane and 1,1,1,3,3,5,5-heptamethyltrisiloxane chains [30–32]. The oligosiloxane-introduced liquid crystals tend to exhibit a thermodynamically stable smectic phase, due to nanosegregation of the oligosiloxane moieties from rigid core units. However, only one report on triphenylene derivatives bearing oligosiloxane chains concerning a columnar liquid crystal has been published [33]. A 1,3,3,5,5,7,7-heptamethylcyclotetrasiloxane ring has yet to be studied as a side chain of liquid crystal materials.

Perylene bisimide is a typical pigment that shows various colors depending upon the aggregation of the π-conjugated units [37–40]. Alkylated perylene bisimide derivatives are used as *n*-type organic semiconductors. Vacuum-deposited thin films of dialkylperylene bisimide derivatives were applied to field-effect transistors [41]. Because of low solubility and inferior processability, thin-film deposition using solution processes is usually difficult.

Oligosiloxane-functionalized perylene bisimide could be synthesized by a hydrosilylation reaction catalyzed by the Karstedt catalyst in good yields [42]. In contrast to conventional perylene bisimide derivatives, the oligosiloxane-introduced perylene bisimide derivatives were highly soluble in organic solvents, such as *n*-hexane, ether, dichloromethane, acetone, and so on, although they are insoluble in methanol and ethanol. They exhibited columnar phases over wide temperature ranges, including room temperature, and their liquid crystalline thin films could be produced by a spin-coating method. Crude products obtained from the reaction mixtures were purified by column chromatography and repeated reprecipitation from methanol [43,44].

2.2. Soft Columnar Phases of the Perylene Bisimide Derivatives Bearing Oligosiloxane Chains

Perylene bisimide derivatives bearing 1,1,1,3,3-pentamethyldisiloxane chains exhibited ordered columnar phases at room temperature [45,46]. Compound **1** (Figure 1a) exhibited a hexagonal ordered columnar phase between 138 °C and 47 °C, at which it transitioned to a rectangular ordered columnar phase. Compound **1** exhibited a glass transition at −56 °C and did not crystallize even when it was cooled to −100 °C. Figure 1b,c exhibit the X-ray diffraction patterns of compound **1** at 30 °C and 70 °C, indicating rectangular and hexagonal ordered columnar phases, respectively. The lattice constants estimated from the diffraction pattern were 21.9 Å and 38.4 Å in the rectangular columnar phase and 22.2 Å in the hexagonal columnar phase. These values are shorter than the molecular size of compound **1**, namely, 32 Å, with a fully extended conformation. A halo around $2\theta \sim 15°$ indicated liquid-like packing of disiloxane chains. The wide-angle diffraction peak at $2\theta = 25°$ indicated a periodic π-π stacking structure within the columnar aggregates. These results indicate that the disiloxane chains should interdigitate to form a core–shell structure, in which one-dimensional crystal-like π-stacks were surrounded by liquid-like siloxane mantle [46].

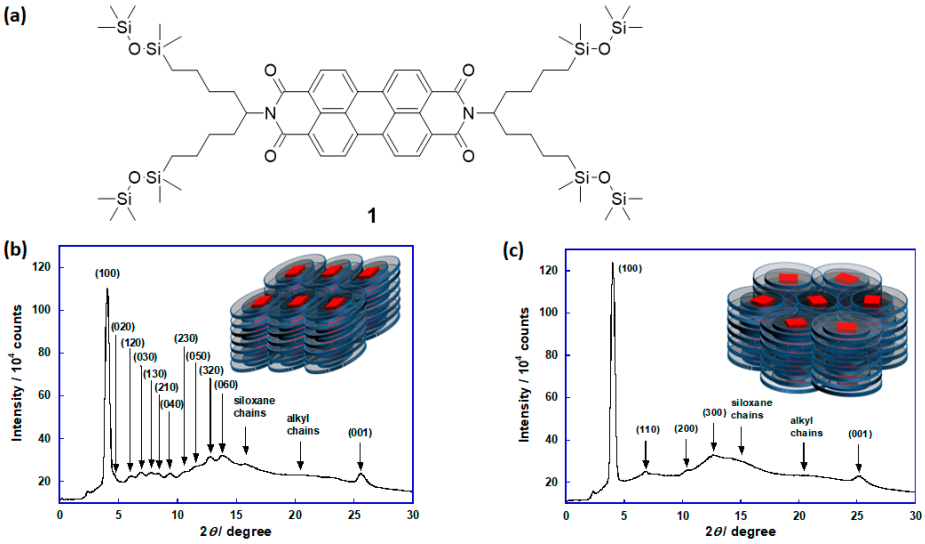

Figure 1. (**a**) Molecular structure of compound **1** and X-ray diffraction patterns of compound **1** at (**b**) 30 °C and (**c**) 70 °C. Insets are schematics for supramolecular aggregation structures at 30 °C and 70 °C. Reproduced from [46], with permission from the Royal Society of Chemistry, 2012.

We synthesized fluorinated analog **2** bearing 1,1,1,3,3-pentamethyldisiloxane chains, as shown in Figure 2a [47]. Figure 2b exhibits an X-ray diffraction pattern of compound **2** at room temperature. Compound **2** also exhibited a hexagonal ordered columnar phase at room temperature. The lattice constant was 22.0 Å in the hexagonal columnar phase. This value was shorter than the molecular size of compound **2** with a fully extended

conformation. A halo around $2\theta \sim 15°$ was also observed, indicating liquid-like packing of disiloxane chains. The wide-angle diffraction peak at $2\theta = 25°$ indicated a periodic π-π stacking structure within the columnar aggregates. As compound **1**, a core–shell structure in which one-dimensional crystal-like π-stacks were surrounded by a liquid-like siloxane mantle in the columnar phase of compound **2**.

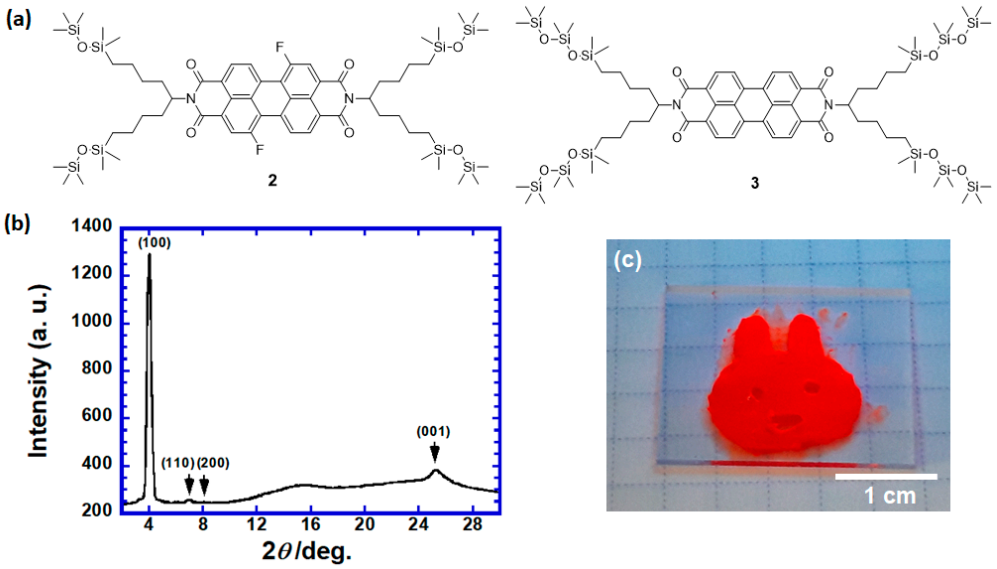

Figure 2. (**a**) Molecular structures of compounds **2** and **3**. (**b**) X-ray diffraction pattern of compound **2** at room temperature. (**c**) The appearance of compound **2**, illuminated by UV light at room temperature. Reproduced from [47], with permission from Elsevier, 2024.

The appearance of the rectangular columnar phase of compound **1** at room temperature was a fine red powder when the material was precipitated in methanol. After melting the red powder and cooling it to room temperature, red soft solids that could be pressed by a spatula were obtained, but they could not be deformed like clay. In contrast, the hexagonal ordered columnar phase of compound **2** at room temperature was much softer than the rectangular ordered columnar phase of compound **1** at room temperature. Compound **2** could be deformed by a spatula like clay, as shown in Figure 2c. It should be noted that the ordered columnar structure based on π-stacks existed in the hexagonal columnar phase of compound **2** at room temperature. Compound **3** bearing four 1,1,1,3,3,5,5-heptamethyltrisiloxane chains (Figure 2a) was also deformable at room temperature. However, the columnar phase of compound **3** was a disordered columnar phase, which did not have a periodical π-π stacking structure within the columnar aggregates [47].

2.3. Nanostructures of Perylene Bisimide and Difluoroperylene Bisimide Derivatives

Surface morphologies of spin-coated films of compounds **1** and **2** in the columnar phases were studied by atomic force microscopy (AFM) [47]. Figure 3 shows height images of the columnar phases of compounds **1** and **2**. A spin-coated film of compound **1** had a surface morphology with an uneven pattern with a periodicity of 500 ~ 700 nm. A stripe pattern with a periodicity of around 50 ~ 100 nm was observed in each convex part with a height of 6 ~ 9 nm, as shown in Figure 3a. The periodicity of the stripe patterns should correspond to that of bundles of the columnar aggregates. The stripes bent at the center of the convex parts at an angle of 18 degrees. This zig-zag bend should be related to the structure of the rectangular columnar phase, in which the normal of the perylene bisimide core is tilted from the columnar axis.

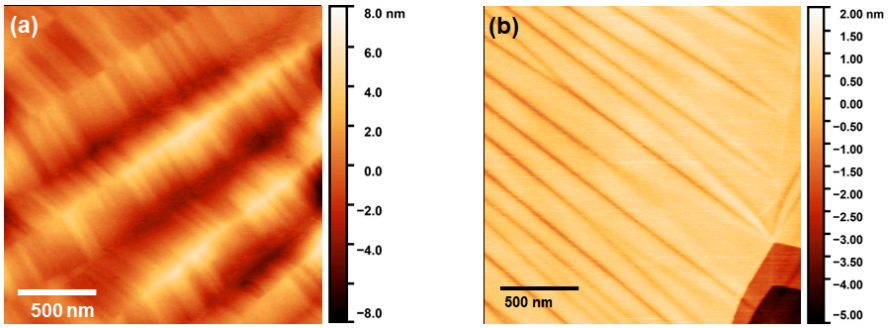

Figure 3. AFM height images of the spin-coated thin films of (**a**) compound **1** and (**b**) compound **2**. Reproduced from [47], with permission from Elsevier, 2024.

In the spin-coated films of compound **2**, stripe patterns on a nanometer scale observed in the films of compound **1** were not formed. The surface morphology of thin films of compound **2** was homogeneous, and any fine structures on a nanometer scale were not observed on the film surface. However, some grooves were formed, as indicated in Figure 3b. The depth and width of the grooves were around 1 nm and 100 nm, respectively. The extraordinary softness of the columnar phase of compound **2** should be induced by the formation of these characteristic nanogrooves. The nanogrooves should be related to mesoscopic voids, which function as free volume for molecular motion.

2.4. Electron Transport in the Soft Columnar Phases of the Perylene Bisimide Derivatives

Measurements of temperature- and field-dependence of a charge carrier mobility over wide temperature and field ranges are required for the determination of a carrier transport mechanism in organic semiconductors. However, the mesomorphic temperature ranges of liquid crystalline semiconductors are usually narrow for discussion on the carrier transport mechanism. Therefore, the electron transport mechanism in liquid crystal phases has not been discussed. Perylene bisimide derivatives bearing oligosiloxane moieties exhibit exceptionally wide mesomorphic temperature ranges, and they are suitable for studies on electron transport in the liquid crystal phases.

Efficient electron transport was confirmed in the columnar phases of compound **1** over a wide temperature range, including room temperature, by the time-of-flight (TOF) technique [46,48,49]. Figure 4a shows transient photocurrent curves for electrons in the rectangular ordered columnar phase at room temperature. Non-dispersive transient photocurrents with plateaus lasting several μs indicated that photogenerated electrons moved with constant velocities over 25 μm. The electron mobility was estimated to be 0.1 $cm^2V^{-1}s^{-1}$ at room temperature. This value was on the same order as aromatic molecular crystals such as anthracene.

Figure 4b shows the electron mobility as a function of temperature. The high electron mobility around 0.1 $cm^2V^{-1}s^{-1}$ was retained between 10 °C and 50 °C, and it decreased with the temperature above 50 °C, due to thermal fluctuation of the columnar aggregates. Below 10 °C, the electron mobility decreased with the decrease in temperature. This behavior should be attributed to a thermal excitation process from deep states to the transport level in the density of states (DOS) in the electron hopping transport. From the temperature- and field-dependence of the electron mobility, disorder parameters could be determined based on the one-dimensional Gaussian disorder model [48]. Compound **3**, bearing bulkier trisiloxane chains, exhibited two orders of magnitude lower electron mobility than that of compound **1** because the mesophase of compound **3** was a hexagonal disordered phase [45].

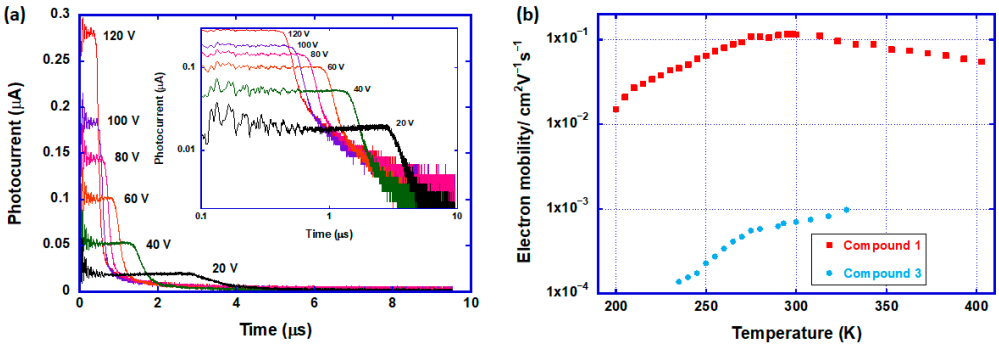

Figure 4. (**a**) Transient photocurrent curves for electrons in the rectangular ordered columnar phase of compound **1** at room temperature in a 25 μm thick cell. (**b**) Electron mobilities of compounds **1** (red) and **3** (light blue) as a function of temperature. Reproduced from [48], with permission from the Royal Society of Chemistry, 2014.

In the hexagonal ordered columnar phase of compound **2**, non-dispersive electron transport was observed by the TOF method, as shown in Figure 5a [47]. The electron mobility was 2×10^{-2} $cm^2V^{-1}s^{-1}$ and depended weakly on the temperature. This value was one order of magnitude lower than that in the ordered columnar phase of compound **1** and one order of magnitude higher than that in the disordered columnar phase of compound **3** bearing four trisiloxane chains. Compound **2** had polar two C-F bonds, and the disordered orientation of the polar bonds in the columnar aggregates should expand the DOS for the electron transport, causing the weak temperature-dependence of the electron mobility as shown in Figure 5b. However, intermolecular π-orbital overlap was retained in the columnar phase, compared to the disordered columnar phase of compound **3**.

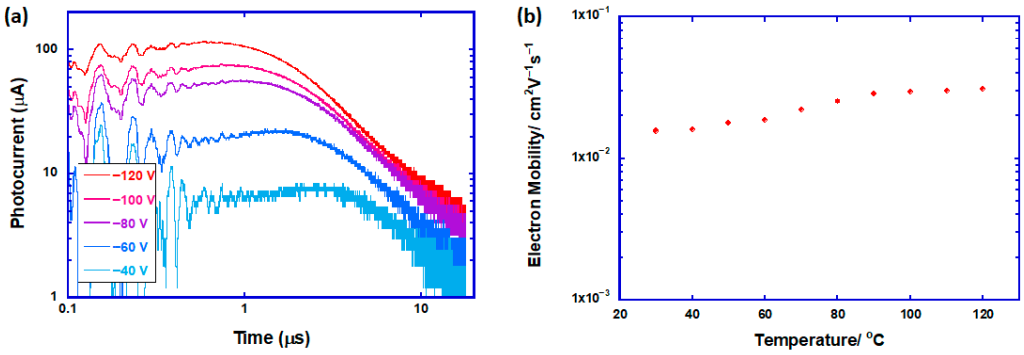

Figure 5. (**a**) Transient photocurrent curves for electrons in the rectangular ordered columnar phase of compound **2** at room temperature in a 15 μm thick cell. (**b**) Electron mobilities of compound **2** as a function of temperature. Reproduced from [47], with permission from Elsevier, 2024.

It should be noted that the efficient electron transport proceeded in the soft columnar phases of compounds **1** and **2**. The efficient electron transport supports the presence of the one-dimensional π-stacks within the columnar aggregates in these columnar phases of compounds **1** and **2**. In particular, compound **2** has exceptional softness. Structural fluctuation is unfavorable for efficient electron transport. However, this soft columnar structure should thermally anneal defects to inhibit the electron transport.

2.5. Polymerizable Perylene Bisimide Derivatives Bearing Cyclotetrasiloxane Moieties

The perylene bisimide moiety functions not only as an electroactive unit but also as a redox-active site. To utilize a perylene bisimide unit for electrochemical materials, redox-active perylene bisimide unit ion-conductive sites should be arranged on a nanometer

scale. Moreover, polymerizable moieties are indispensable for the insolubilization of the materials, because they are usually used in organic electrolyte solutions.

We have paid attention to cyclotetrasiloxane rings polymerizing via a ring-opening mechanism. Moreover, the cyclotetrasiloxane ring is a bulky substituent to inhibit aggregation of π-conjugated cores and promote nanosegregation in the formation of liquid crystal phases, although cyclotetrasiloxane rings have not been used as a side chain moiety.

We synthesized compound **4** bearing four 1,3,3,5,5,7,7-heptamethylcyclotetrasiloxane rings, as shown in Figure 6a [50]. Compound **4** exhibited a hexagonal disordered columnar phase below 72.3 °C. Figure 6b exhibits an X-ray diffraction pattern in the columnar phase of compound **4** at room temperature. Similarly to compounds **1** and **2**, the shorter lattice constant than the molecular size indicated interdigitation of side chains to form a core–shell structure in the columnar phase. The diffraction pattern lacked a peak derived from π-π stacking of the perylene bisimide units around 25°, indicating a disordered columnar phase, which was unfavorable for efficient electron transport. However, the electron mobility in the disordered columnar phase reached 0.1 $cm^2V^{-1}s^{-1}$ at room temperature, as shown in Figure 6c,d. Despite the bulkiness of a cyclotetrasiloxane ring and the absence of periodicity within columnar aggregates, this high electron mobility indicated large π-orbital overlaps in the columnar phase.

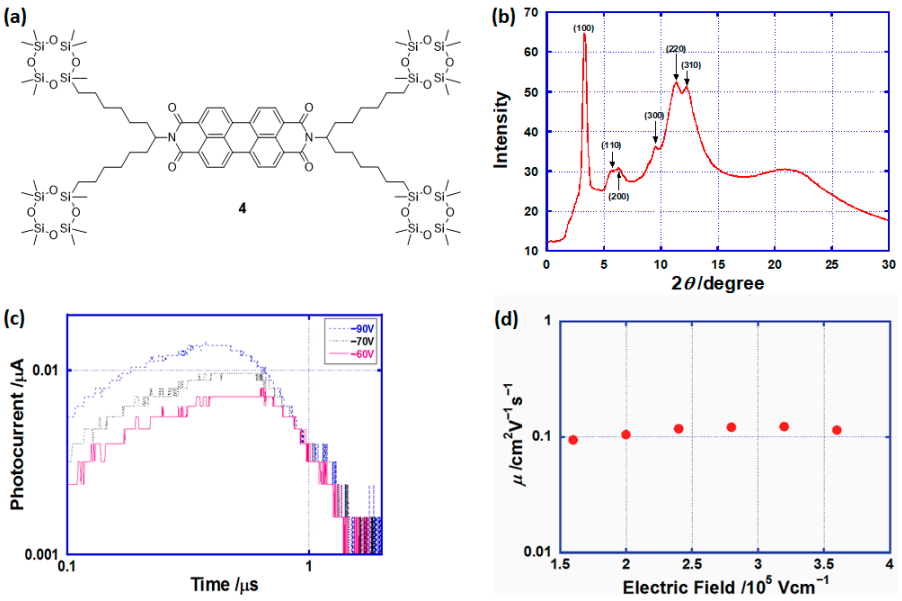

Figure 6. (**a**) Molecular structure of compound **4**. (**b**) X-ray diffraction pattern of compound **4** at room temperature. (**c**) Transient photocurrent curves for electrons at room temperature using a 25 μm thick cell. (**d**) Electron mobility in the columnar phase of compound **4** at room temperature as a function of the electric field. Reproduced from [49], with permission from the Royal Society of Chemistry, 2016.

Another characteristic feature of compound **4** is ring-opening polymerization catalyzed by acid vapor in thin film states. Octamethyltetrasiloxane polymerizes in a solution state in the presence of acidic or basic catalyst via a ring-opening mechanism. Compound **4** polymerized in organic solvents under acidic conditions to generate insoluble precipitates because of the generation of network polymers. The polymerized products were insoluble in organic solvents and could not be purified. Therefore, polymerized thin films could not be deposited on substrates by a spin-coating or a solution-casting method.

However, compound **4** was soluble in various organic solvents except for alcohols, and liquid crystalline thin films could be deposited by a spin-coating method. The spin-coated film was insolubilized by exposure to trifluoromethanesulfonic acid vapors at 70 °C for

5 min, as shown in Figure 7a [51]. The acid vapors should diffuse into the spin-coated film, inducing ring-opening polymerization.

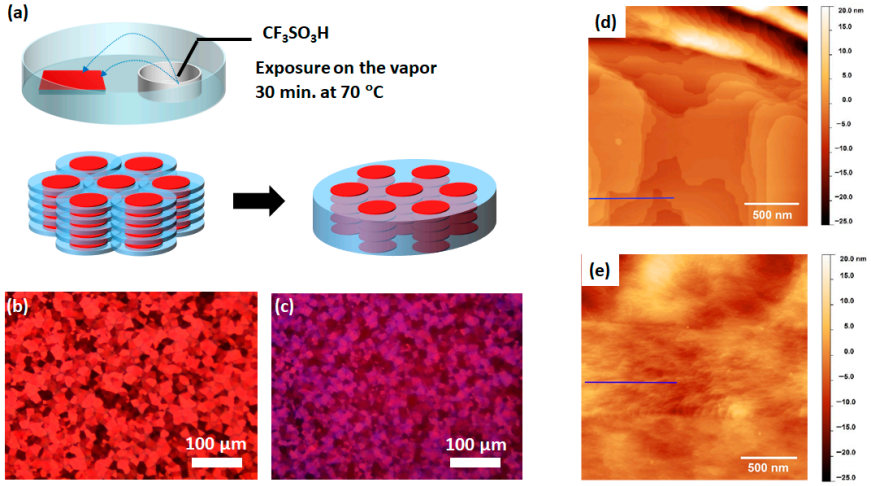

Figure 7. (**a**) Illustration of in situ acid-vapor-induced ring-opening polymerization in a thin film state. Polarizing optical micrographic textures of a spin-coated film of compound **4** (**b**) before and (**c**) after the in situ polymerization. AFM height images of spin-coated thin films of compound **4** (**d**) before and (**e**) after the in situ polymerization. Reproduced from [49], with permission from the Royal Society of Chemistry, 2016.

As shown in Figure 7b,c, the polarizing micrographic textures of the thin film did not change before and after polymerization, indicating the macroscopic molecular alignment was retained during the in situ polymerization. However, fine structures of the thin film on a nanometer scale could not be retained during the in situ polymerization process. Figure 7d,e show the height images of the thin film of compound **3** before and after the in situ polymerization. On the surface of the as-deposited film, terrace structures were observed with a step height of 2.0 nm, which was comparable to the diameter of the columnar aggregates of 2.4 nm. On the surface of the thin film after the in situ polymerization, only ambiguous uneven structures were formed, indicating increased structural disorder of the columnar aggregates by ring-opening of tetrasiloxane rings [51].

3. Perylene Bisimide Derivatives Bearing Oligoether Moieties as Well as Oligosiloxane Units

3.1. Liquid Crystalline Perylene Bisimide Derivatives Bearing One Triethylene Oxide Chain

For combining the redox activity of perylene bisimide cores with ionic transport, we synthesized perylene bisimide derivatives bearing hydrophilic triethylene oxide chains and crown ether rings. Bart and coworkers have already reported mesomorphic perylene bisimide derivatives bearing oligoethylene oxide chains and enhanced electrical conduction by doping metallic lithium. In our study, thin films of liquid crystalline perylene bisimide could be produced by solution processes and insolubilized in thin film states. Therefore, enhanced conductivity by doping in aqueous solution, anisotropic conductivity, electrochromism, and ion selectivity could be achieved in thin film states.

First, we synthesized compound **5** bearing two disiloxane and one triethylene oxide chains, as shown in Figure 8a [52]. Compound **5** exhibited a smectic phase with a layered structure, unlike other perylene bisimide derivatives bearing four oligosiloxane moieties exhibiting columnar phases. Compound **5** could be hybridized with lithium triflate (LiOTf) up to 3 mol%, due to electrostatic interaction between triethylene oxide chains and lithium cations, as indicated in the DSC thermograms in Figure 8b. In the presence of LiOTf with

1 mol%, transient photocurrent curves were observed by the TOF measurement, although the electron mobility decreased from 1×10^{-3} $cm^2V^{-1}s^{-1}$ to 5×10^{-4} $cm^2V^{-1}s^{-1}$.

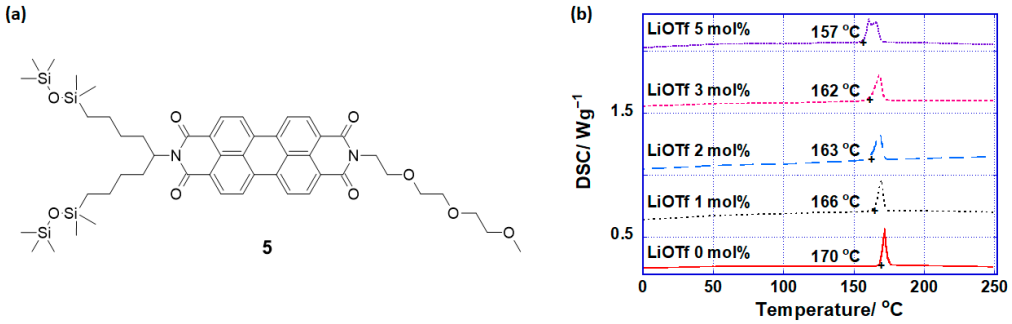

Figure 8. (**a**) Molecular structure of compound **5**. (**b**) DSC thermograms of compound **5** mixed with LiOTf. Reproduced from [52], with permission from the Royal Society of Chemistry, 2013.

We also synthesized perylene bisimide derivatives **6** and **7** bearing two cyclotetrasiloxane rings as well as an alkyl chain or a triethylene oxide chain, as shown in Figure 9a [53]. These compounds exhibited columnar phases at room temperature. However, the nanostructures of the columnar phases of these compounds were quite different. In the columnar phase of compound **6** bearing an alkyl chain, perylene bisimide cores are stacked to form one-dimensional electron transport paths (Figure 9b).

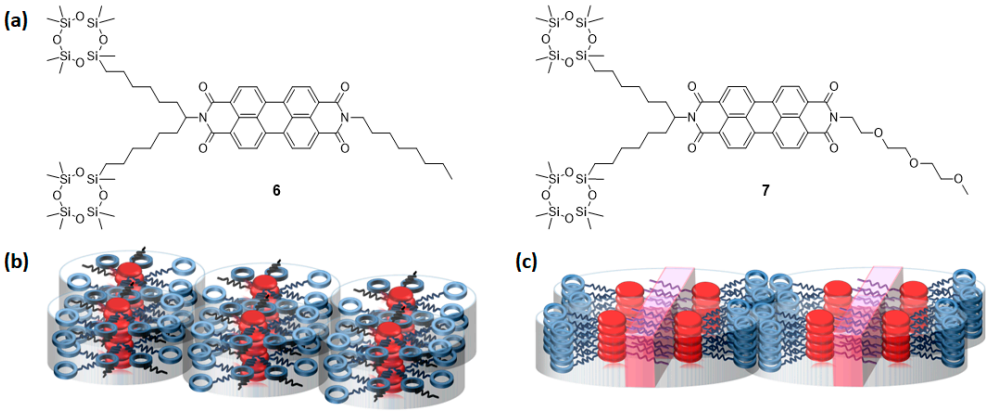

Figure 9. (**a**) Molecular structures of compounds **6** and **7**. Schematics for supramolecular aggregation in the columnar phases of (**b**) compound **6** and (**c**) compound **7**. The areas with hatched with pink color in the columnar aggregates indicate ion-conductive sublayers. Reproduced from [53], with permission from the Royal Society of Chemistry, 2017.

In contrast, the columnar phase of the compound **7** chain had a dimeric structure in which an ion-conductive sublayer as well as one-dimensional π-stacks were formed within a columnar aggregate, due to hydrophilic interaction between triethylene oxide chains (Figure 9c). These compounds were soluble in various organic solvents except for alcohols, and thin films could be produced by a spin-coating method. On friction-transferred substrates, uniaxially aligned thin films could be deposited [53].

3.2. Anisotropic Optical and Electronical Properties of Thin Films

A rubbing method using a polyimide alignment layer is effective to orient LC molecules in a nematic and smectic A phases in one direction. However, it is generally difficult to produce uniaxially aligned films of ordered smectic phases and columnar phases.

A friction transfer method is a kind of graphoepitaxy technique and is effective to align conjugated polymers and phthalocyanine nanowires in a vacuum deposition

process [54–56]. This method is also effective for producing uniaxially aligned columnar LC thin films by the spin-coating method. In this method, a Teflon block is pressed on a heated substrate over 150 °C, which moves in one direction. A solution of columnar liquid crystal is spun on the substrate on which uniaxially aligned Teflon nanofibers are adhered (Figure 10a). Figure 10b shows polarized UV-vis absorption spectra of as-deposited uniaxially aligned films of compound **7**. The absorption perpendicular to the friction direction was fifteen times larger than that parallel to the friction direction. The columnar axis was parallel to the friction direction, and the transition moments of perylene bisimide cores were perpendicular to the columnar axis. The anisotropy in the absorption was decreased to 4:1 in the polymerized film (Figure 10c). This decreased anisotropy should be attributed to the increased structural disorder during the polymerization [53].

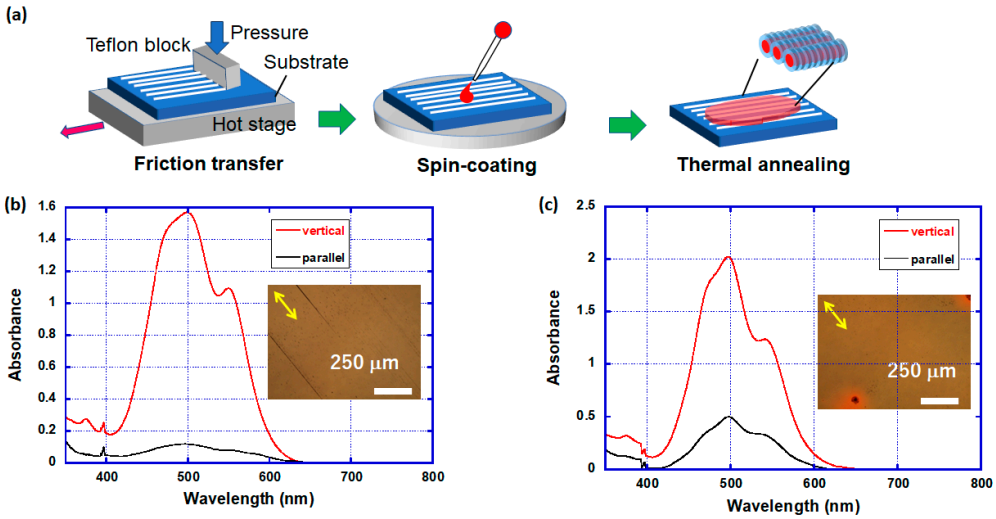

Figure 10. (**a**) Illustration of a friction transfer method for the production of uniaxially aligned thin films. Polarized UV-Vis absorption spectra of uniaxially aligned thin films of compound **7** in (**b**) the initial and (**c**) polymerized states. Red and black lines indicate the spectra polarized vertical and parallel to the friction direction, respectively. Insets indicate polarizing optical micrographs of uniaxially aligned spin-coated thin films of compound **7** before and after in situ polymerization. Yellow arrows indicate the axes of polarizers. Reproduced from [53], with permission from the Royal Society of Chemistry, 2017.

As shown in Figure 9c, it is noted that the ion-conductive sublayers are within the columnar aggregates of compound **7**. When a spin-coated film of compound **7** was dipped in an aqueous solution of sodium dithionate, sodium cations and reductant dithionate anions could penetrate into the thin film and dithionate anions reduced perylene bisimide cores, changing the color of the thin film from red to blue-violet, as shown in Figure 11a. In the polymerized thin films, the same color change was observed by the treatment with sodium dithionate solution. This color change indicated the generation of dianions of perylene bisimide units. On the other hand, a spin-coated film of compound **6** did not indicate such a color change by the treatment of a sodium dithionate solution [53].

In the columnar phases of compounds **6** and **7**, the TOF measurement revealed the electron mobilities on the order of 10^{-2} and 10^{-3} $cm^2V^{-1}s^{-1}$, respectively. An anisotropic electrical conductivity was studied for uniaxially aligned doped thin films of compounds **6** and **7**. Under an inert gas atmosphere, the spin-coated film was dipped in a sodium dithionate solution. The electrical conductivities along and perpendicular to the columnar axis were determined, using substrates with patterned electrodes, as shown in Figure 11b.

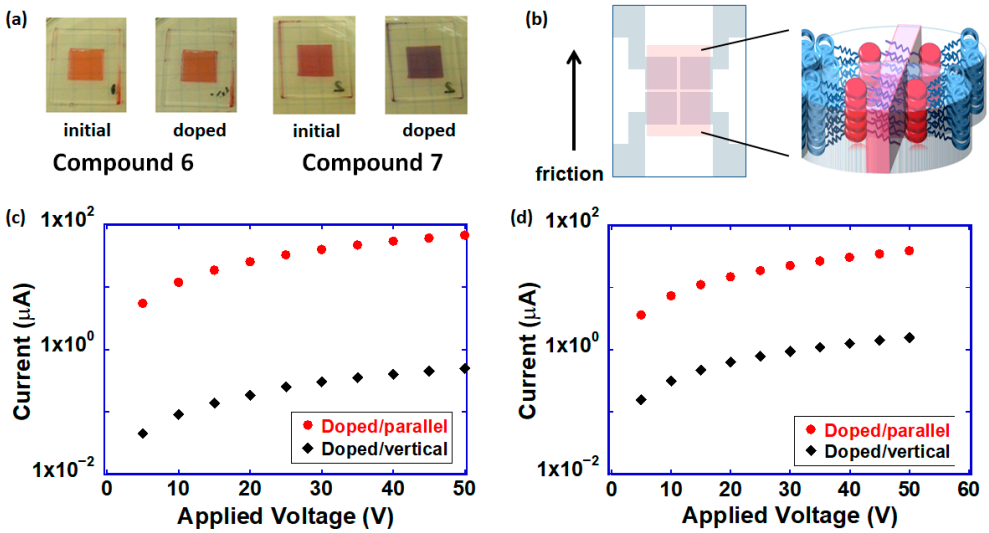

Figure 11. (**a**) Photographs of non-doped and doped thin films of compounds **6** and **7**. (**b**) The patterned electrodes for the measurement of anisotropic electrical conductivity. Current–voltage characteristics of the uniaxially aligned thin film of compound **7** (**c**) before and (**d**) after the in situ polymerization. Reproduced from [53], with permission from the Royal Society of Chemistry, 2017.

In the case of the thin film of compound **7**, the electrical conductivity along the columnar axis was 1×10^{-10} S·cm^{-1} in a neutral state, but it increased to 3×10^{-4} S·cm^{-1} after dipping in the reductant solution. However, the conductivity of the thin film of compound **6** indicated a little change from the order of 10^{-10} S·cm^{-1} to the order of 10^{-8} S·cm^{-1} by the treatment. The enhancement of the conductivity should be attributed to the generation of anion radicals formed in perylene bisimide units. This behavior should be an interstitial doping, in which the dopant ions are located within the ion-conductive sublayers consisting of triethylene oxide chains [53].

Figure 11c shows current–voltage characteristics of the uniaxially aligned thin films treated with sodium dithionate solution. The electrical conductivity parallel and perpendicular to the columnar axis was 3×10^{-4} and 1×10^{-6} S·cm^{-1}, respectively. Anisotropy of the electrical conductivity should be attributed to the anisotropy of the electron mobility in the columnar phase. This method was effective for polymerized uniaxially aligned films. The electrical conductivity along the columnar axis for a doped film was 2×10^{-4} S·cm^{-1}, although the anisotropy of the conductivity decreased around 10 (Figure 11d) [53].

3.3. Perylene Bisimide Derivatives Bearing Crown Ether Rings

Compound **7** bearing one triethylene oxide chain was hybridized with LiOTf up to 5 mol%. To increase the concentration of alkaline metal salts in the LC perylene bisimide derivatives, we synthesized perylene bisimide derivatives **8** and **9** bearing a crown ether unit as well as cyclotetrasiloxane rings (Figure 12) [57,58]. Crown-ether-based liquid crystals have been studied extensively by Laschat and coworkers [59]. However, their crown-ether-based liquid crystals did not comprise electroactive groups.

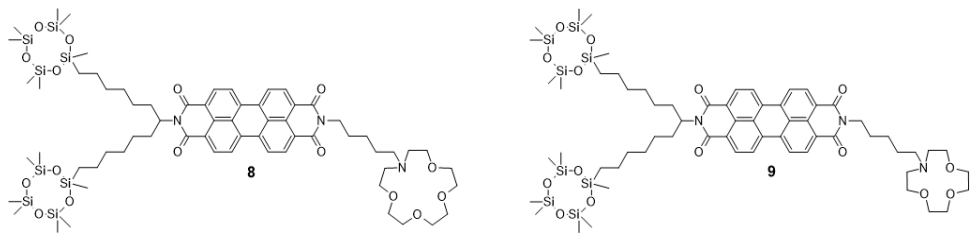

Figure 12. Molecular structures of perylene bisimide derivatives bearing a crown ether ring.

Compound **8** exhibited a rectangular ordered columnar phase at room temperature, as shown in Figure 13a,b [57]. In the columnar phase, molecules of compound **8** stacked in an antiparallel manner to form columnar aggregates, which were arranged in a rectangular lattice. It is noted that a (001) diffraction peak indicating π-π stacking in the columnar aggregates appeared despite the presence of bulky cyclotetrasiloxane and crown ether rings. Figure 13c shows the phase transition temperature of compound **8** and its complex with LiOTf and NaOTf as a function of the triflate concentration. The 1:1 mixture of compound **8** with LiOTf, as well as NaOTf, exhibited a homogenous columnar phase at room temperature, indicating the formation of a 1:1 complex, while compounds **5** and **7** bearing a triethylene oxide chain could not form 1:1 complexes. Electrostatic interaction between crown-lithium or crown-sodium cations and triflate anions stabilized the 1:1 complex thermodynamically, resulting in the increased phase transition temperature of the complex. For KOTf, a homogenous phase was not formed due to the segregation of KOTf.

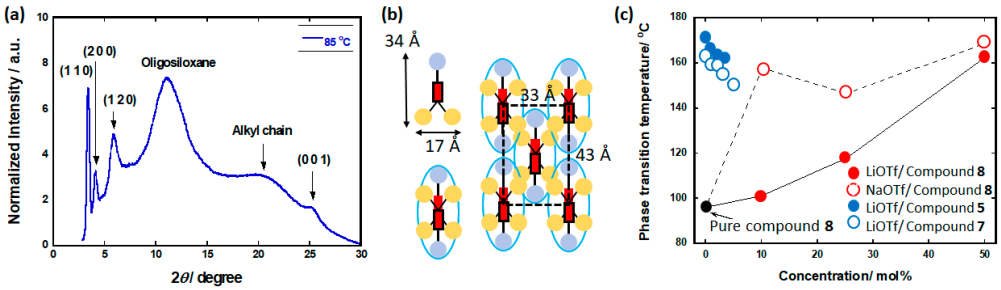

Figure 13. (**a**) X-ray diffraction pattern of the columnar phase of compound **8** at 80 °C and (**b**) schematic for the supramolecular structure of the columnar phase. (**c**) Phase transition temperature of the complexes of compound **8** with LiOTf and NaOTf, and mixtures of compounds **5** and **7** with LiOTf. Reproduced from [57], with permission from the Royal Society of Chemistry, 2022.

3.4. Nanostructures of Perylene Bisimide Derivatives Bearing a Crown Ether Ring

The spin-coated films of compound **8** and its complexes indicated characteristic nanostructures [57]. The surface morphology of compound **8** itself exhibited flat domains with a size of 1 ~ 2 μm without fine structures, as shown in Figure 14a. In the equimolar mixture of compound **8** and KOTf, flat domains with a size of several μm were also exhibited (Figure 14b). However, bending stripes were observed on the surface morphology of 1:1 complexes with LiOTf and NaOTf (Figure 14c,d). In the thin film of 1:1 complex with LiOTf, the periodicity of the stripe pattern was 6 nm, which coincided with the lattice constant of the complex. For the thin film of the complex with NaOTf, the periodicity was 21 nm, indicating the formation of bundles of columnar aggregates. In these complexes, the electrostatic interaction between positively charged crown rings and triflate anions should promote the formation of bundles of the columnar aggregates.

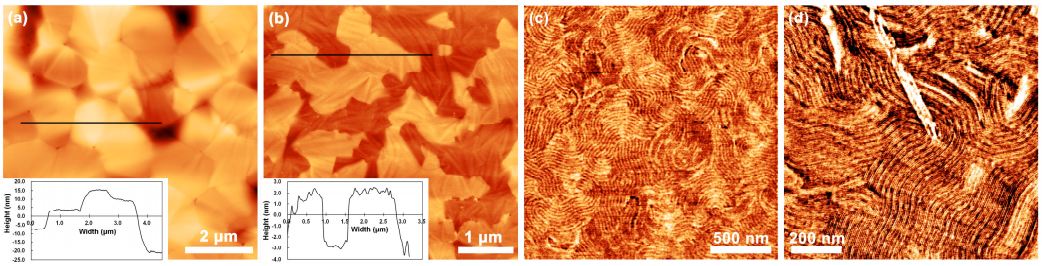

Figure 14. AFM height images of the spin-coated thin films of (**a**) compound **8** and (**b**) its equimolar mixture of compound **8** and KOTf. The insets indicate surface height profiles along the black lines. AFM phase images of 1:1 complexes of compound **8** with (**c**) LiOTf and (**d**) NaOTf. Reproduced from [57], with permission from the Royal Society of Chemistry, 2022.

Compound **9**, having a smaller 12-crown-4 ring, also formed a 1:1 complex with LiOTf, while it does not form a well-defined complex with NaOTf [58]. Compound **9** itself exhibited an extraordinarily linear periodic stripe structure over 1 μm on the surface morphology (Figure 15a). In the surface morphology of the 1:1 complex with LiOTf, well-defined bent stripes with a periodicity of 7 nm were formed (Figure 15b). However, the periodic structure was ambiguous in the surface morphology of the equimolar mixture with NaOTf, as shown in Figure 15c. In the case of LiOTf, the size of the lithium cation matched the size of the 12-crown-4 ring to form stoichiometric 1:1 complexes, resulting in the well-defined stripe structure in the surface morphology. In contrast, an equilibrium mixture of non-coordinated compound **9** and the 1:1 and 1:2 complexes should be formed, leading to the ambiguous nanostructure in the surface morphology.

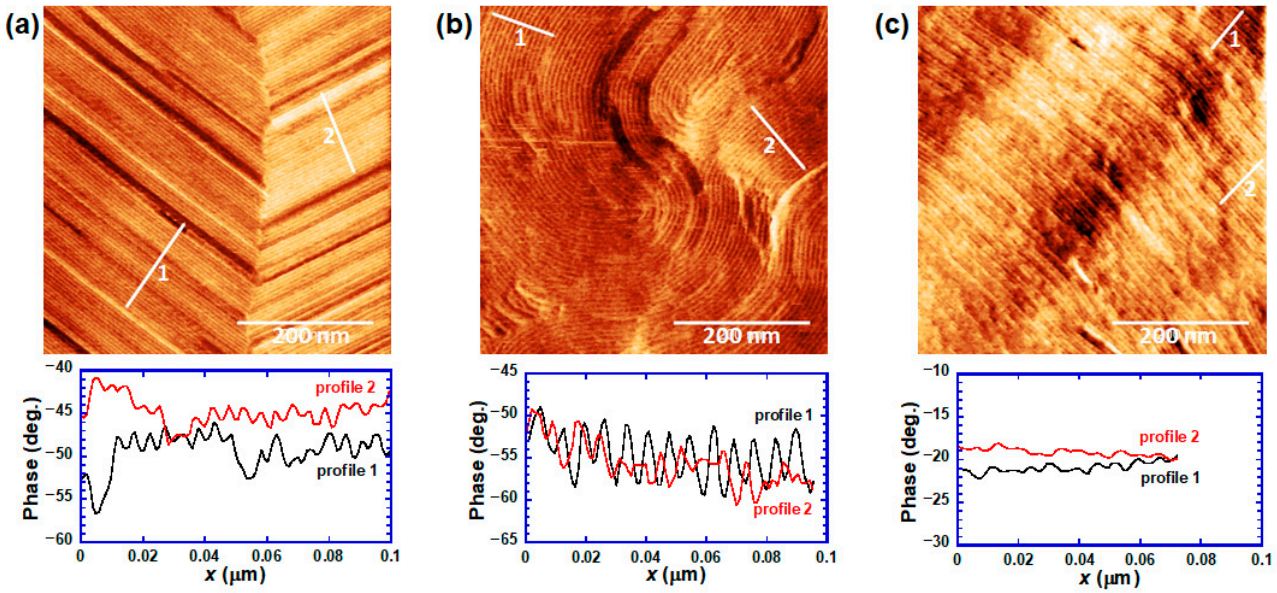

Figure 15. AFM phase images and phase profiles along the white lines of the spin-coated films of (**a**) compound **9**, (**b**) 1:1 complex of compound **9** with LiOTf, and (**c**) equimolar mixture of compound **9** and NaOTf. Reproduced from [58], with permission from the Chemical Society of Japan, 2026.

Spin-coated thin films could be insolubilized by the in situ polymerization by exposure to trifluoromethanesulfonic acid vapors at 60 °C. The nanostructures in the surface morphologies of the spin-coated films of compounds **8** and **9** were not retained during the in situ acid-vapor-catalyzed ring-opening polymerization (Figure 16a,d), due to the conformation change in the oligosiloxane moieties [58]. However, the nanostructures for 1:1 complexes of compound **8**, with LiOTf and NaOTf, and of compound **9**, with LiOTf, formed well-defined stripe patterns, which were maintained during the in situ ring-opening polymerization (Figure 16b,e,f). The ambiguous stripe pattern of the complex of compound **8** and NaOTf was not retained during the polymerization (Figure 16c). These behaviors should be attributed to the enhanced stability of the nanostructures by electrostatic interaction between positively charged crown rings and triflate anions.

3.5. Electrochemical Properties of Perylene Bisimide Derivatives Bearing a Crown Ether Ring

The spin-coated films of compound **8** were insolubilized by the in situ ring-opening polymerization, and they could be used in organic electrolyte solutions. The polymerized thin film exhibited electrochromism between red color in a neutral state and blue-violet in a dianion state under a negative bias application in organic electrolyte solutions [57]. Figure 17a shows a cyclic voltammogram of the polymerized thin film of compound **8** in an acetonitrile solution (LiOTf 1 M). Scanning between 0 and −1.5 V vs. an Ag^+/Ag standard

electrode, redox peaks originated from the generation of radical anions and dianions were observed, although the separation between one-electron and two-electron reduction processes was not sufficient. Figure 17b presents UV-vis absorption spectra of the polymerized thin film deposited on an ITO electrode in an acetonitrile solution containing 1M LiOTf. In the electrochemical reduction, anion radicals with absorption peaks at 720 nm and 810 nm were generated first, and then dianions with absorption peaks at 530 nm and 620 nm were produced. Figure 17c exhibits the reversible electrochromic response of the polymerized thin film of compound **8** in a LiOTf solution. In NaOTf solution, the polymerized thin film exhibited the same behavior. However, the electrochromic response was not persistent in a tetrabutylammonium perchlorate solution. In the polymerized films of compound **8**, ion channels should be formed by the aggregation of crown rings, and lithium and sodium cations could penetrate reversibly. On the other hand, tetrabutylammonium cations had a larger size than that of the ion channels consisting of the crown rings and could not penetrate into the thin films. Repeated application of the negative bias caused decomposition of the thin films.

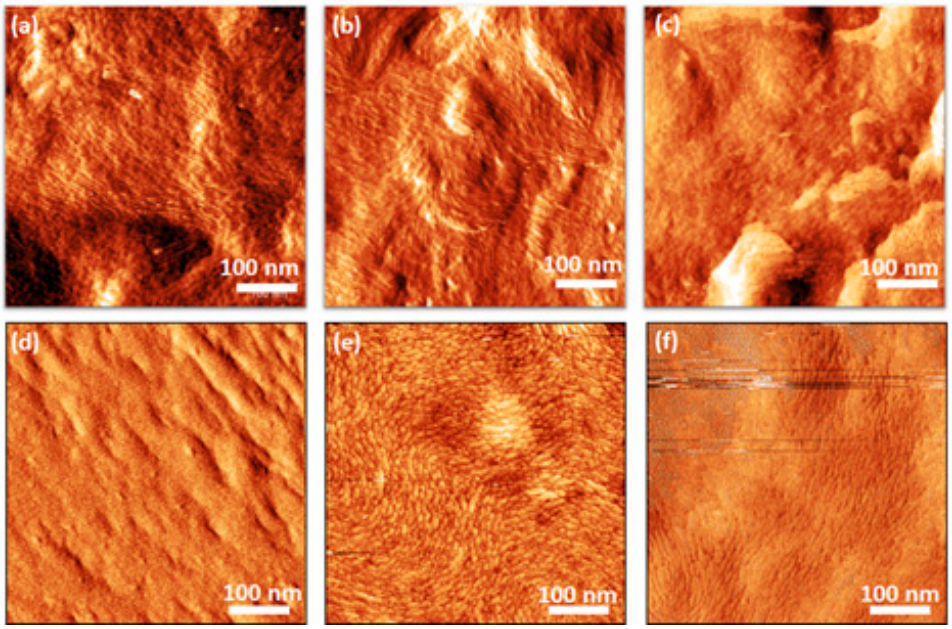

Figure 16. AFM phase images of the polymerized spin-coated thin film of (**a**) compound **9**, (**b**) 1:1 complex of compound **9** with LiOTf, (**c**) equimolar mixture of compound **9** and NaOTf, (**d**) compound **8**, (**e**) 1:1 complex of compound **8** with LiOTf, and (**f**) 1:1 complex of compound **8** with NaOTf. Reproduced from [58], with permission from the Chemical Society of Japan, 2026.

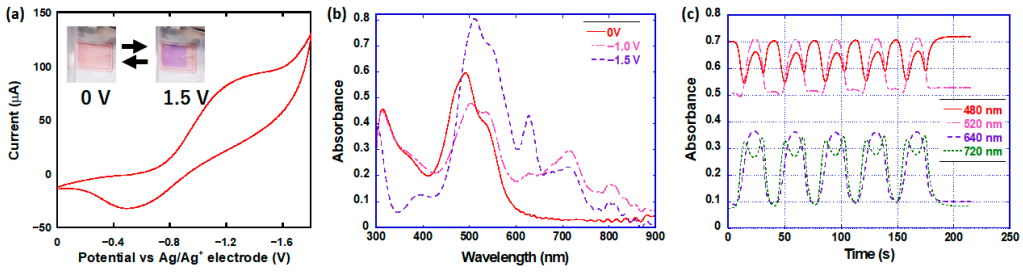

Figure 17. (**a**) A cyclic voltammogram, (**b**) UV-Vis absorption spectra, and (**c**) electrochromic response of the polymerized spin-coated film of compound **8** in an acetonitrile solution of LiOTf (1 M). Reproduced from [57], with permission from the Royal Society of Chemistry, 2022.

4. Related Materials

Figure 18 exhibited the other examples of mesomorphic perylene bisimide derivatives bearing oligosiloxane chains. Dibenzyl perylene bisimide derivative **10** bearing oligosiloxane chains was reported, and the material exhibited a columnar phase with a helical structure at room temperature. In the columnar phase of compound **10**, electron mobility was determined to be 1.5×10^{-3} $cm^2V^{-1}s^{-1}$ [60]. Polymer **11**, consisting of perylene bisimide units and oligosiloxane chains, also exhibited a mesophase at room temperature. Photoconductivity in the thin films of polymer **11** was studied [61].

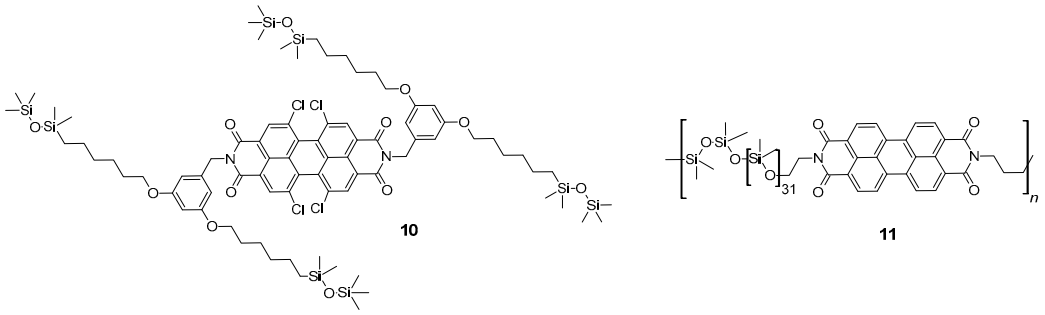

Figure 18. Molecular structures of related compounds consisting of perylene bisimide units and oligosiloxane chains.

5. Conclusions

Oligosiloxane side chains are effective to promote self-organization of π-conjugated units to form crystal-like electronic carrier transporting paths surrounded by a liquid-like mantle consisting of oligosiloxane moieties. As a result, soft electronic systems with waxy appearances were constructed, which indicated high electron mobilities on the order of $10^{-2} \sim 10^{-1}$ $cm^2V^{-1}s^{-1}$ over wide temperature ranges, including room temperature. These compounds are highly soluble in organic solvents, and thin films could be produced by the spin-coating method. In particular, spin-coated thin films of the perylene bisimide derivatives bearing cyclotetrasiloxane rings were insolubilized by exposure to trifluoromethanesulfonic acid vapors via the in situ ring-opening polymerization. Perylene bisimide derivatives bearing a triethylene oxide chain as well as cyclotetrasiloxane rings exhibited increased electrical conductivity by interstitial doping in an aqueous solution of sodium dithionate. Uniaxially aligned thin films exhibited anisotropic electrical conductivity. The conductivity along and parallel to the columnar axis in the non-polymerized state was 10^{-4} and 10^{-6} $S{\cdot}cm^{-1}$, respectively. Polymerized thin films of perylene bisimide derivatives bearing a crown ether ring as well as cyclotetrasiloxane rings exhibited reversible electrochromism between the neutral and dianion states in electrolyte solutions. These compounds formed 1:1 complexes with lithium triflate, exhibiting columnar phases at room temperature. The nanostructures of the complexes were stabilized by the electrostatic interaction between cationic crown-metal units and triflate anions, and they were retained during the in situ ring-opening polymerization. Oligosiloxane moieties are *convenient* side chains for the construction of soft nanosegregated electronic systems with electronic and electrochemical functions.

Funding: This study was financially supported by a Grant-in-Aid for Scientific Research on Innovative Areas (Element-Block Polymers, No. 15H00753) from the Ministry of Education, Culture, Sports, Science and Technology (MEXT), a Grant-in-Aid for Scientific Research (B) (No. 15H03797, 21H01904) from the Japan Society for the Promotion of Science (JSPS), the Asahi Glass Foundation, the Salt Science Research Foundation (No. 1715), the Iketani Science and Technology Foundation, the Japan Keirin Autorace Foundation (2022M-221) and the Nankai Ikuei Foundation. This research was also

supported by the 'Nanotechnology Platform Program' of the Ministry of Education, Culture, Sports, Science and Technology (MEXT), Japan (Grant No. JPMXP09F19GA0004).

Data Availability Statement: No new data were created or analyzed in this study. Data sharing is not applicable to this article.

Acknowledgments: The authors thank Tomohiko Ishii for X-ray diffraction analysis and Takafumi Kusunose for DSC measurements. The authors also thank Mika Yamaoka, Kaede Takenami, Shunsuke Takaoka, Kurumi Suemoto, Daiki Taga, Tatsumitsu Kajiwara, and all students of the Funahashi group in Kagawa University for their collaboration in the research.

Conflicts of Interest: The authors declare no conflicts of interest.

References

1. O'Neill, M.; Kelly, S.M. Ordered Materials for Organic Electronics and Photonics. *Adv. Mater.* **2011**, *23*, 566–584. [CrossRef]
2. Kato, T.; Yoshio, M.; Ichikawa, T.; Soberats, B.; Ohno, H.; Funahashi, M. Transport of ions and electrons in nanostructured liquid crystals. *Nat. Rev. Mater.* **2017**, *2*, 17001. [CrossRef]
3. Funahashi, M. Nanostructured Liquid-Crystalline Semiconductors—A New Approach to Soft Matter Electronics. *J. Mater. Chem. C* **2014**, *2*, 7451–7459. [CrossRef]
4. Funahashi, M. Solution-processable electronic and redox-active liquid crystals based on the design of side chains. *Flex. Print. Electron.* **2020**, *5*, 043001. [CrossRef]
5. Funahashi, M. Chiral Liquid Crystalline Electronic Systems. *Symmetry* **2021**, *13*, 672. [CrossRef]
6. Adam, D.; Schuhmacher, P.; Simmerer, J.; Häussling, L.; Siemensmeyer, K.; Etzbach, K.H.; Ringsdorf, H.; Haarer, D. Fast photoconduction in the highly ordered columnar phase of a discotic liquid crystal. *Nature* **1994**, *371*, 141–143. [CrossRef]
7. Fleischmann, E.-K.; Zentel, R. Liquid-Crystalline Ordering as a Concept in Materials Science: From Semiconductors to Stimuli-Responsive Devices. *Angew. Chem. Int. Ed.* **2013**, *52*, 8810–8827. [CrossRef]
8. Funahashi, M.; Ishii, T.; Sonoda, A. Temperature-Independent Hole Mobility of a Smectic Liquid-Crystalline Semiconductor based on Band-Like Conduction. *ChemPhysChem* **2013**, *14*, 2750–2758. [CrossRef]
9. Aldred, M.P.; Contoret, A.E.A.; Farrar, S.R.; Kelly, S.M.; Mathieson, D.; O'Neill, M.; Tsoi, W.C.; Vlachos, P. A Full Color Electroluminescence Device and Patterned Photoalignment Using Light Emitting Liquid Crystal. *Adv. Mater.* **2005**, *17*, 1368–1372. [CrossRef]
10. Funahashi, M. Development of liquid crystalline semiconductors with high carrier mobility and their application to thin-film transistors. *Polym. J.* **2009**, *41*, 459–469. [CrossRef]
11. Pisula, W.; Menon, A.; Stepputat, M.; Lieberwirth, I.; Kolb, U.; Tracz, A.; Sirringhaus, H.; Pakula, T.; Müllen, K. A Zone Casting Technique for Device Fabrication of Field-Effect Transistors Based on Discotic Hexa-peri-Hexabenzocoronene. *Adv. Mater.* **2005**, *17*, 684–689.
12. van Breemen, A.J.J.M.; Herwig, P.T.; Chlon, C.H.T.; Sweelssen, J.; Schoo, H.F.M.; Setayesh, S.; Hardeman, W.M.; Martin, C.A.; de Leeuw, D.M.; Valeton, J.J.P.; et al. Large area liquid crystal Monodomain field-effect transistors. *J. Am. Chem. Soc.* **2006**, *128*, 2336–2345. [CrossRef] [PubMed]
13. Funahashi, M.; Zhang, F.; Tamaoki, N. High ambipolar mobility in highly ordered smectic phase of dialkylphenylterthiophene derivative that can be applied to solution-processed organic field effect transistors. *Adv. Mater.* **2007**, *19*, 353–358. [CrossRef]
14. Zhang, F.; Funahashi, M.; Tamaoki, N. High-performance thin film transistors from semiconducting liquid crystalline phases by solution processes. *Appl. Phys. Lett.* **2007**, *91*, 063515. [CrossRef]
15. Iino, H.; Usui, T.; Hanna, J. Liquid crystals for organic thin-film transistors. *Nat. Commun.* **2015**, *6*, 6828. [CrossRef]
16. Schmidt-Mende, L.; Fechtenkötter, A.; Müllen, K.; Moons, E.; Friend, R.H.; MacKenzie, J.D. Self-Organized Discotic Liquid Crystals for High-Efficiency Organic Photovoltaics. *Science* **2001**, *293*, 1119–1122. [CrossRef]
17. Hori, T.; Miyake, Y.; Yamasaki, N.; Yoshida, H.; Fujii, A.; Shimizu, Y.; Ozaki, M. Solution Processable Organic Solar Cell Based on Bulk Heterojunction Utilizing Phthalocyanine Derivative. *Appl. Phys. Express* **2010**, *3*, 101602. [CrossRef]
18. Chandrasekhar, S. *Liquid Crystals*; Cambridge University Press: Cambridge, UK, 2010.
19. Kato, T. Self-assembly of phase-segregated liquid crystal structures. *Science* **2002**, *295*, 2414–2418. [CrossRef]
20. Kato, T.; Uchida, J.; Ichikawa, T.; Sakamoto, T. Functional liquid crystals towards the next generation of materials. *Angew. Chem. Int. Ed.* **2018**, *57*, 4355–4371. [CrossRef] [PubMed]
21. Uchida, J.; Soberats, B.; Gupta, M.; Kato, T. Advanced functional liquid crystals. *Adv. Mater.* **2022**, *34*, 2109063.
22. Ichikawa, T.; Yoshio, M.; Hamasaki, A.; Kagimoto, J.; Ohno, H.; Kato, T. 3D interconnected ionic nano-channels formed in polymer films: Self-organization and polymerization of thermotropic bicontinuous cubic liquid crystals. *J. Am. Chem. Soc.* **2011**, *133*, 2163–2169. [CrossRef]

23. Yoneya, M. Toward rational design of complex nanostructured liquid crystals. *Chem. Rec.* **2011**, *11*, 66–76. [CrossRef] [PubMed]
24. Schenning, A.P.H.J.; Kilbinger, A.F.M.; Biscarini, F.; Cavallini, M.; Cooper, H.J.; Derrick, P.J.; Feast, W.J.; Lazzaroni, R.; Leclére, P.; McDonell, L.A.; et al. Supramolecular Organization of α,α′-Disubstituted Sexithiophenes. *J. Am. Chem. Soc.* **2002**, *124*, 1269–1275. [CrossRef]
25. Liu, S.-G.; Sui, G.; Cormier, R.A.; Leblanc, R.M.; Gregg, B.A. Self-Organizing Liquid Crystal Perylene Diimide Thin Films: Spectroscopy, Crystallinity, and Molecular Orientation. *J. Phys. Chem. B* **2002**, *106*, 1307–1315. [CrossRef]
26. Kishimoto, K.; Yoshio, M.; Mukai, T.; Yoshizawa, M.; Ohno, H.; Kato, T. Nanostructured anisotropic ion-conductive films. *J. Am. Chem. Soc.* **2003**, *125*, 3196–3197. [CrossRef]
27. Mei, J.; Kim, D.H.; Ayzner, A.L.; Toney, M.F.; Bao, Z. Siloxane-Terminated Solubilizing Side Chains: Bringing Conjugated Polymer Backbones Closer and Boosting Hole Mobilities in Thin-Film Transistors. *J. Am. Chem. Soc.* **2011**, *133*, 20130–20133. [CrossRef]
28. Fujita, K.; Sumino, Y.; Ide, K.; Tamba, S.; Shono, K.; Shen, J.; Nishino, T.; Mori, A.; Yasuda, T. Synthesis of Poly(3-substituted thiophene)s of Remarkably High Solubility in Hydrocarbon via Nickel-Catalyzed Deprotonative Cross-Coupling Polycondensation. *Macromolecules* **2016**, *49*, 1259–1269. [CrossRef]
29. Ogura, T.; Kubota, C.; Suzuki, T.; Okano, K.; Tanaka, N.; Matsumoto, T.; Nishino, T.; Mori, A.; Okita, T.; Funahashi, M. Synthesis and Properties of Regioregular Polythiophene Bearing Cyclic Siloxane Moiety at the Side Chain and the Formation of Polysiloxane Gel by Acid Treatment of the Thin Film. *Chem. Lett.* **2019**, *48*, 611–614. [CrossRef]
30. Lagarwall, J.P.F.; Giesselmann, F. Current Topics in Smectic Liquid Crystal Research. *ChemPhysChem* **2006**, *7*, 20–45. [CrossRef] [PubMed]
31. Apreutesei, D.; Mehl, G. The design and investigation of laterally functionalised oxadiazoles. *J. Mater. Chem.* **2007**, *17*, 4711–4715. [CrossRef]
32. Newton, J.; Coles, H.; Hodge, P.; Hannington, J. Synthesis and properties of low-molar-mass liquid-crystalline siloxane derivatives. *J. Mater. Chem.* **1994**, *4*, 869–874. [CrossRef]
33. Zelcer, A.; Donnio, B.; Bourgogne, C.; Cukiernik, F.D.; Guillon, D. Mesomorphism of Hybrid Siloxane-Triphenylene Star-Shaped Oligomers. *Chem. Mater.* **2007**, *19*, 1992–2006. [CrossRef]
34. Dankert, F.; von Hänisch, C. Siloxane Coordination Revisited: Si-O Bond Character, Reactivity and Magnificent Molecular Shapes. *Eur. J. Inorg. Chem.* **2021**, *29*, 2907–2927. [CrossRef]
35. Auner, N.; Weis, J. *Organosilicon Chemistry II, From Molecules to Materials*; VCH: Weinheim, Germany, 1996.
36. Matsui, A.; Funahashi, M.; Tsuji, T.; Kato, T. High Hole Mobility for a Side-Chain Liquid-Crystalline Smectic Polysiloxane Exhibiting a Nanosegregated Structure with a Terthiophene Moiety. *Chem. Eur. J.* **2010**, *16*, 13465–13472. [CrossRef]
37. Langhals, H. Control of the interactions in multichromophores: Novel concepts. Perylene bis-imides as components for larger functional units. *Helv. Chim. Acta* **2005**, *88*, 1309–1343. [CrossRef]
38. Chen, Z.; Baumeister, U.; Tschierske, C.; Würthner, F. Effect of Core Twisting on Self-Assembly and Optical Properties of Perylene Bisimide Dyes in Solution and Columnar Liquid Crystalline Phases. *Chem. Eur. J.* **2007**, *13*, 450–465.
39. Hecht, M.; Schlossarek, T.; Stolte, M.; Lehmann, M.; Würthner, F. Photoconductive Core-Shell Liquid-Crystals of a Perylene Bisimide J-Aggregate Donor-Acceptor Dyad. *Angew. Chem. Int. Ed.* **2019**, *58*, 12979–12983. [CrossRef]
40. Würthner, F.; Saha-Möller, C.R.; Fimmel, B.; Ogi, S.; Leowanawat, P.; Schmidt, D. Perylene Bisimide Dye Assemblies as Archetype Functional Supramolecular Materials. *Chem. Rev.* **2016**, *116*, 962–1052. [CrossRef] [PubMed]
41. Jeon, H.-G.; Hattori, J.; Kato, S.; Oguma, N.; Hirata, N.; Taniguchi, Y.; Ichikawa, M. Thermal treatment effects on *N*-alkyl perylene diimide thin-film transistors with different alkyl chain. *J. Appl. Phys.* **2010**, *108*, 124512.
42. Karstedt, B.D. Platinum Complexes of Unsaturated Siloxanes and Platinum Containing Organopolysiloxanes. U.S. Patent 3,775,452, 27 November 1973.
43. Funahashi, M. Integration of electro-active π-conjugated units in nanosegregated liquid-crystalline phases. *Polym. J.* **2017**, *49*, 75–83.
44. Funhahashi, M. Electrochemical Functions of Nanostructured Liquid Crystals with Electronic and Ionic Conductivity. In *Advances in Organic Crystal Chemistry*; Sakamoto, M., Uekusa, H., Eds.; Springer Nature: Singapore, 2020; pp. 359–377.
45. Funahashi, M.; Sonoda, A. Liquid-crystalline perylene tetracarboxylic acid bisimide bearing oligosiloxane chains with high electron mobility and solubility. *Org. Electron.* **2012**, *13*, 1633–1640.
46. Funahashi, M.; Sonoda, A. High electron mobility in a columnar phase of liquid-crystalline perylene tetracarboxylic bisimide bearing oligosiloxane chains. *J. Mater. Chem.* **2012**, *22*, 25190–25197. [CrossRef]
47. Funahashi, M.; Uemura, S. Carrier transport and mesomorphic properties of deformable fluorinated perylene bisimide bearing disiloxane chains. *J. Mol. Liq.* **2024**, *407*, 125267. [CrossRef]
48. Funahashi, M.; Sonoda, A. Electron transport characteristics in nanosegregated columnar phases of perylene tetracarboxylic bisimide derivatives bearing oligosiloxane chains. *Phys. Chem. Chem. Phys.* **2014**, *16*, 7754–7763. [CrossRef]
49. Funahashi, M.; Takeuchi, N.; Sonoda, A. A liquid-crystalline perylene tetracarboxylic bisimide derivative bearing trisiloxan-2-yl moieties: Influence on mesomorphic properties and electron transport. *RSC Adv.* **2016**, *6*, 18703–18710. [CrossRef]

50. Funahashi, M.; Yamaoka, M.; Takenami, K.; Sonoda, A. Liquid-crystalline perylene tetracarboxylic bisimide derivatives bearing cyclotetrasiloxane moieties. *J. Mater. Chem. C* **2013**, *1*, 7872–7878. [CrossRef]
51. Takenami, K.; Uemura, S.; Funahashi, M. In situ polymerization of liquid-crystalline thin films of electron-transporting perylene tetracarboxylic bisimide bearing cyclotetrasiloxane rings. *RSC Adv.* **2016**, *6*, 5474–5484.
52. Funahashi, M.; Sonoda, A. A liquid-crystalline perylene tetracarboxylic bisimide derivative bearing a triethylene oxide chain and complexation of the derivative with Li cations. *Dalton Trans.* **2013**, *42*, 15987–15994. [CrossRef]
53. Funahashi, M. Anisotropic electrical conductivity of n-doped thin films of polymerizable liquid-crystalline perylene bisimide bearing a triethylene oxide chain and cyclotetrasiloxane rings. *Mater. Chem. Front.* **2017**, *1*, 1137–1146.
54. Wittmann, J.C.; Smith, P. Highly oriented thin films of poly(tetrafluoroethylene) as a substrate for oriented growth of materials. *Nature* **1991**, *352*, 414–417. [CrossRef]
55. Ueda, Y.; Kuriyama, T.; Hari, T.; Ashida, M. Crystal growth and molecular orientation of organic materials vapor-deposited on highly-oriented polytetrafluoroethylene thin film. *J. Electron. Microsc.* **1994**, *43*, 99–103.
56. Chiyonobu, Y.; Koshiba, Y.; Tomosada, K.; Matsumoto, T.; Horike, S.; Nishino, T.; Ishida, K.; Funahashi, M. Preparation of thin films with densely aggregated zinc phthalocyanine nanowires oriented uniaxially on friction-transferred polytetrafluoroethylene template. *Discov. Polym.* **2025**, *2*, 8. [CrossRef]
57. Taga, T.; Takaoka, S.; Uemura, S.; Funahashi, M. Liquid-crystalline perylene bisimide derivatives bearing an azacrown ether ring complexing with alkaline metal ions. *Mater. Chem. Front.* **2022**, *6*, 880–890. [CrossRef]
58. Kajiwara, T.; Taga, T.; Akiyama, A.; Koshiba, Y.; Horike, S.; Kirikawa, K.; Uemura, S.; Funahashi, M. Nanostructures of liquid crystalline thin films of perylene bisimide derivatives bearing a 12-crown-4 ring complexing with lithium triflate. *Bull. Chem. Soc. Jpn.* **2026**, *99*, uoag016. [CrossRef]
59. Steinke, N.; Frey, W.; Baro, A.; Laschat, S.; Drees, C.; Nimtz, M.; Högele, C.; Gießelmann, F. Columnar and Smectic Liquid Crystals Based on Crown Ethers. *Chem. Eur. J.* **2006**, *12*, 1026–1035. [CrossRef]
60. Zeng, Y.; Lu, L.; Gao, T.; Feng, Y.; Zheng, J.-F.; Chen, E.-Q.; Ren, X.-K. Synthesis, helical columnar liquid crystalline structure, and charge transporting property of perylene diimide derivative bearing oligosiloxane chains. *Dye. Pigment.* **2018**, *152*, 139–145. [CrossRef]
61. Iwan, A.; Schab-Balcerzak, E.; Pociecha, D.; Krompiec, M.; Grucela, M.; Bilski, P.; Kłosowski, M.; Janeczek, H. Characterization, liquid crystalline behavior, electrochemical and optoelectrical properties of new poly(azomethine)s and a poly(imide) with siloxane linkages. *Opt. Mater.* **2011**, *34*, 61–74. [CrossRef]